

1 **Title:**

2 **Increased region of surround stimulation**
3 **enhances contextual feedback and feedforward**
4 **processing in human V1**

5 **Abbreviated title:** How context enhances cortical feedback to V1

6
7 **Author names and affiliations:**

8 Yulia Revina^{1*}

9 Lucy S. Petro¹

10 Cristina B. Denk-Florea¹

11 Isa S. Rao¹

12 Lars Muckli^{1,2}

13 ¹ Centre for Cognitive Neuroimaging, Institute of Neuroscience & Psychology, University of
14 Glasgow, G12 8QB, Glasgow, United Kingdom.

15 ² Imaging Centre of Excellence, College of Medical, Veterinary and Life Sciences, University of
16 Glasgow and Queen Elizabeth University Hospital, G51 4LB, Glasgow, United Kingdom.

17 **Email addresses:** yurevina@cbs.mpg.de (YR); lucy.petro@glasgow.ac.uk (LSP); c.denk-
18 florea.1@research.gla.ac.uk (CBD-F); isa.rao@gmx.de (ISR); Lars.Muckli@glasgow.ac.uk (LM)

19 **Corresponding Author:** Lars Muckli, 62 Hillhead Street, Glasgow, G12 8QB, UK.
20 Lars.Muckli@glasgow.ac.uk

21
22 **Number of pages:** 31

23 **Number of figures:** 6

24 **Number of tables:** 4

25 **Number of words | Abstract:** 190

26 **Number of words | Introduction:** 628

27 **Number of words | Discussion:** 1493

28 **Conflict of interest:** The authors declare no competing financial interests.

29 **Acknowledgements:** This work was supported by the European Research Council grant (ERC
30 StG 2012_311751-‘Brain reading of contextual feedback and predictions’ awarded to LM) and
31 BBSRC DTP Studentship (YR). This project has received funding from the European Union’s
32 Horizon 2020 Framework Programme for Research and Innovation under the Specific Grant

33 Agreement No. 720270, 785907, and 945539 (Human Brain Project SGA1-3). We thank Frances
34 Crabbe for assistance with data collection.

35 *Author YR current affiliation: Max Planck Institute for Human Cognitive and Brain Sciences,
36 Leipzig, Germany.

37

38

39 Abstract

40 The majority of synaptic inputs to the primary visual cortex (V1) are non-feedforward, instead
41 originating from local and anatomical feedback connections. Animal electrophysiology
42 experiments show that feedback signals originating from higher visual areas with larger receptive
43 fields modulate the surround receptive fields of V1 neurons. Theories of cortical processing
44 propose various roles for feedback and feedforward processing, but systematically investigating
45 their independent contributions to cortical processing is challenging because feedback and
46 feedforward processes coexist even in single neurons. Capitalising on the larger receptive fields
47 of higher visual areas compared to primary visual cortex (V1), we used an occlusion paradigm
48 that isolates top-down influences from feedforward processing. We utilised functional magnetic
49 resonance imaging (fMRI) and multi-voxel pattern analysis methods in humans viewing natural
50 scene images. We parametrically measured how the availability of contextual information
51 determines the presence of detectable feedback information in non-stimulated V1, and how
52 feedback information interacts with feedforward processing. We show that increasing the visibility
53 of the contextual surround increases scene-specific feedback information, and that this contextual
54 feedback enhances feedforward information. Our findings are in line with theories that cortical
55 feedback signals transmit internal models of predicted inputs.

56 Significance Statement

57 The visual system has circuit mechanisms for processing scene context. These circuits involve
58 lateral and feedback inputs to neurons. These inputs interact with feedforward inputs and
59 modulate neuronal responses to visual stimuli presented outside their receptive fields.
60 Systematically investigating independent contributions of feedback and feedforward processes is
61 challenging because they coexist even in single neurons. Here we use an occlusion paradigm to
62 isolate feedback and lateral signals in human participants viewing natural scene images in fMRI.
63 We show that increasing the visibility of the contextual surround increases scene-specific
64 feedback information, which also enhances feedforward signals. Our findings are in line with
65 theories that cortical feedback signals carry abstract internal models that combine with more
66 detailed representations in primary visual cortex.

67

68 Introduction

69 Sensory stimulation triggers a cascade of processing in a hierarchy of visual areas. This
70 feedforward processing meets recurrent activity from the previous sensory input and triggers
71 recurrent activity that will meet the next expected visual input. Recurrent processing
72 contextualises and predicts the incoming signal and updates internal models and future recurrent
73 streams. The contextualisation of feedforward information by feedback signals is essential for our
74 understanding of cortical processing (Gilbert and Li, 2011). We know from animal recordings that
75 cortical neurons are contextually modulated when their response to a feedforward stimulus
76 feature is modified by the presence of surrounding features (Sugita, 1999; Shushruth, 2011). In
77 visual cortex, this contextual information can be located far in the surround of a neuron's
78 receptive field. Consequently, contextual modulation of neurons is exerted by cortical feedback
79 and lateral inputs (Angelucci, 2002). Cortical feedback inputs, at least in non-human primate
80 cortex, arrive to discrete portions of cortical pyramidal neurons; mainly to the apical dendrites
81 that branch up to layer 1 (Douglas and Martin, 2007). Feedback inputs are therefore

82 computationally distinct from feedforward inputs arriving to basal dendrites. Recent conceptual
83 shifts in our understanding of neuronal computation are contributing to a developing perspective
84 on the significance of cortical feedback inputs in determining neuronal information processing
85 (Larkum, 2013). This perspective requires techniques to probe brain processing that detect
86 neuronal inputs, advancing previous studies that mainly measure neuronal outputs (i.e. spiking
87 activity Larkum et al., 2018; Muckli et al., 2015). Functional magnetic resonance imaging (fMRI)
88 is one such technique that detects pre- and postsynaptic inputs, offering a means to measure
89 contextual feedback information to a region of cortex.

90 Understanding the nature of contextual modulation transmitted by cortical feedback and
91 lateral interaction is vital for understanding the brain in behavioural and cognitive contexts
92 (Gilbert and Sigman, 2007). This importance of cortical feedback and lateral interaction arises
93 because contextual modulations on a neuron include influences from higher-level top-down
94 processes including expectation, prior experience and goal-directed behaviour, which originate in
95 higher cortical areas (Muckli and Petro, 2013). Therefore, describing neuronal substrates of
96 cognition in brain networks including sensory areas requires us to measure not only stimulus-
97 driven neuronal responses under discrete states of top-down influences (e.g. attention,
98 expectation, task, working memory), but also feedback-driven responses in isolation from
99 feedforward processing. Measuring feedback-driven modulations separate from stimulus-driven
100 activity allows us to investigate the information contained in top-down influences. These signals
101 alter neuronal responses to stimuli (Li et al., 2004; Schwiedrzik and Freiwald, 2017; Petro and
102 Muckli, 2018), which may depend on other state variables (e.g. being conscious, Philips et al.,
103 2016), therefore functionally determining the brain's response to its environment (Friston, 2010;
104 Clark, 2015).

105 We used fMRI, a brain imaging measure of energy consumption, and multivoxel pattern
106 analysis (MVPA) to investigate how global natural scene features contextually modulate human
107 V1. Our approach complements non-classical receptive field studies in rodent and monkey cortex,
108 that measure spikes in response to a feedforward stimulus relative to contextual surround

109 stimulation. However, the proposed tuning to pre-and post-synaptic activity in apical dendrites
110 that might be detectable by fMRI allows us to capitalise on a signal that might not always be
111 available in sharp electrode electrophysiology, where the input at the apical dendrites might not
112 lead to a change in spiking output. Using partially occluded images, we parametrically vary the
113 amount of global contextual information that we provide and measure the resulting contextual
114 feedback (and lateral interaction) information to V1 both in the absence of feedforward
115 information, and when feedback is integrated with feedforward information. If global features in
116 the surround contextually modulate human V1, we hypothesized that scene information in non-
117 feedforward-stimulated V1 voxels should decrease with progressive masking of the surround, and
118 increased surround stimulation should modulate detectable scene information even when V1
119 voxels receive feedforward stimulation.

120

121 Materials and Methods

122 Subjects

123 We compensated twenty-nine subjects from the University of Glasgow to participate in the
124 experiment (n = 13 males; mean age: 24.28 years, range: 19-41 years). Subjects provided informed
125 written consent and the experiment was approved by the local ethics committee at the University
126 of Glasgow (CSE01063). We excluded subjects if their data was at chance level classification
127 performance in at least one feedforward control condition (n = 5) or poorly aligned (anatomically)
128 between functional runs (n = 3, see *Voxel Selection and Analysis*, indicating substantial body
129 movement between scans). Below we report results from 21 subjects with stable classification in
130 feedforward control conditions (n = 10 males; mean age: 25.29 years, range 19-41 years).

131 Stimuli

132 Feedback vs Feedforward condition

133 We used occluded natural scene stimuli to investigate cortical feedback signals in the
134 absence of feedforward stimulation (Smith and Muckli, 2010; Muckli et al., 2015; Revina et al.,
135 2018; Morgan et al., 2019). For the feedback conditions, the lower right image quadrant was

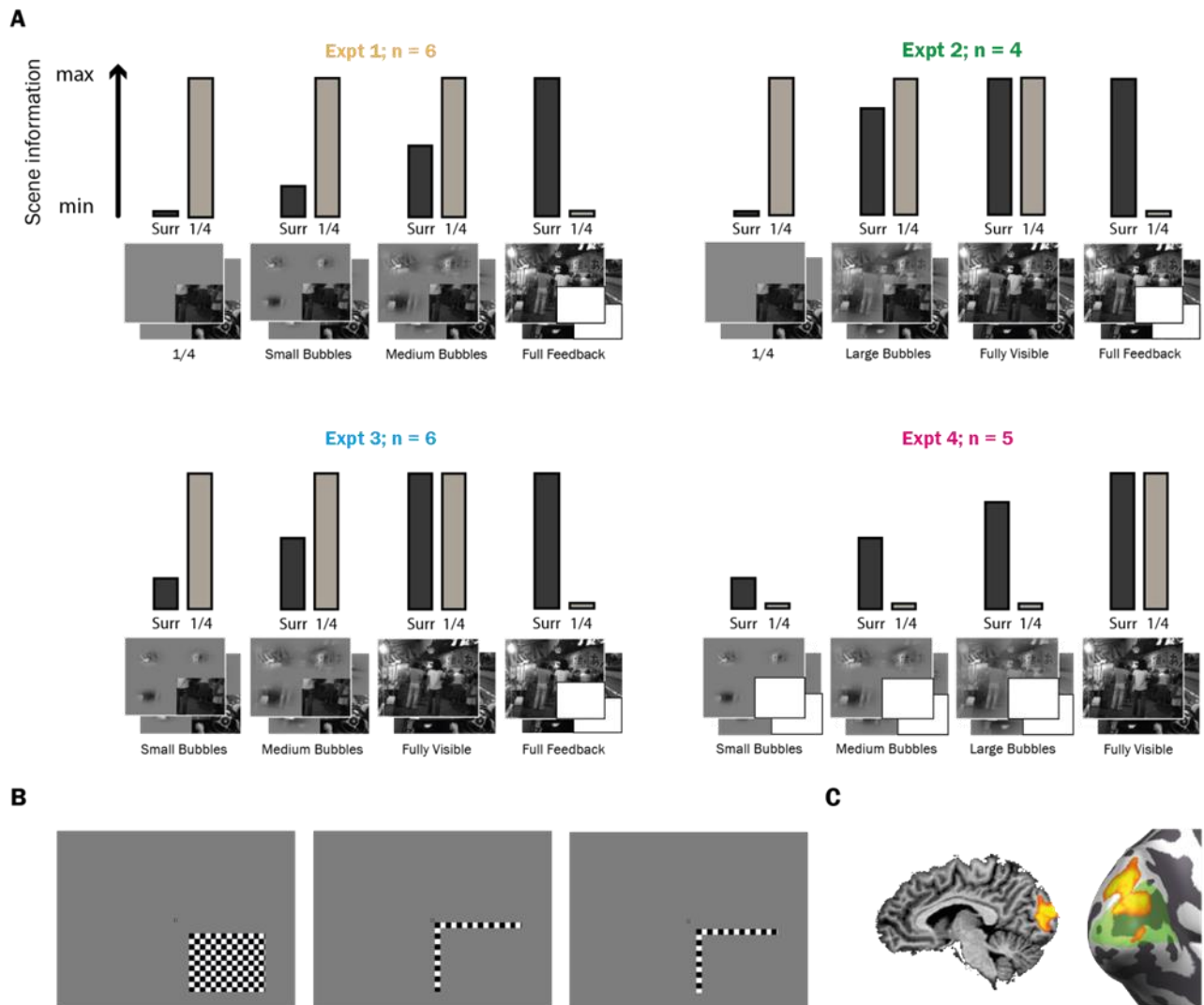
136 occluded by a white rectangle. Here we expect that the retinotopic region of V1 responding to the
137 white portion of the image receives no meaningful feedforward input and only cortical feedback
138 signals (and lateral inputs). The white rectangle was placed 0.5° of visual angle diagonally from
139 the centre of the image and spanned $11.6^\circ \times 9.2^\circ$. In the so-called ‘feedforward’ conditions, the
140 corresponding quadrant of the scene was shown; V1 voxels responding to the lower image
141 quadrant in this condition contain a mixture of feedforward, lateral and feedback inputs.

142 Scenes

143 We used two natural scene images for each participant, as natural scenes induce a lot of
144 contextual associations (Bar 2004). Each scene was 600×480 pixels and spanned $24^\circ \times 19.2^\circ$ of
145 visual angle. We did not normalize the images in terms of low-level visual features, such as
146 luminance, contrast or energy at each spatial frequency because we wanted the scenes to look as
147 natural as possible. Smith and Muckli (2010) previously showed that contextual feedback signals
148 in V1 cannot be solely attributed to these low-level visual features.

149 To investigate the contribution of surrounding contextual information on the brain activity
150 patterns corresponding to the lower right quadrant, we manipulated the visibility of the
151 surrounding $\frac{3}{4}$ of the scene with a Gaussian aperture in each quadrant (“bubbles”, Gosselin and
152 Schyns, 2001) of various sizes to reveal the scene and produce the following types of stimuli: $\frac{1}{4}$
153 (no surrounding scene shown), Small Bubbles (standard deviation [SD] = 50×32 pixels),
154 Medium Bubbles (SD = 90×56 pixels), Large Bubbles (SD = 125×100 pixels) and Full (surround
155 fully visible). The study consisted of four experiments, with each subject participating in only one
156 ($n = 6$; $n = 4$; $n = 6$; $n = 5$ respectively). In each experiment, stimuli were shown in four (out of
157 the five possible) different conditions (**Figure 1A**). In Experiment 1, we used stimuli in the Full
158 Feedback occluded condition, $\frac{1}{4}$ feedforward, Small Bubbles feedforward and Medium Bubbles
159 feedforward conditions. In Experiment 2, we replaced Small and Medium Bubbles with Large
160 Bubbles and the Fully Visible scene. In Experiment 3, we added the Fully Visible scene to test
161 whether more contextual feedback would be seen in the Small and Medium Bubbles conditions if
162 participants were more familiar with the full scene. In Experiment 4, we tested the effect of

163 reducing the surrounding information around the occluded region using Small, Medium and
 164 Large Bubbles feedback conditions.



165 **Figure 1.** Stimuli. A) In feedback conditions the lower right image quadrant was occluded with a white rectangle,
 166 while in feedforward conditions the corresponding quadrant was visible. We manipulated scene visibility around the
 167 lower right quadrant with bubbles of various sizes to create 5 types of conditions: 1/4, Small Bubbles, Medium Bubbles,
 168 Large Bubbles and Full. Dark bars labelled “Surr” illustrate the extent to which the surrounding 3/4 of the scene was
 169 revealed. Light bars labelled “1/4” illustrate the extent to which the lower right image quadrant was revealed. Bars are
 170 not to scale. B) Checkerboard stimuli were used to retinotopically map the occluded region in V1; left to right Target,
 171 Near Surround, Inner Border. C) The activation for the contrast of (Target – Near Surround) used to map non-
 172 stimulated V1 is shown on the occipital cortex on one subject, with V1 in green on the inflated visualization.
 173

174 Occluded region mapping

175 We presented subjects with three contrast-reversing checkerboards (5 Hz) twice per run.
 176 The checkerboards either covered an inner rectangular part of the occluded region (*Target* – 2.5°
 177 diagonally from centre, 10.2° × 7.8° visual angle) or the border between the lower right quadrant
 178 and the rest of the stimulus (*Surround*). There were two types of surround checkerboard stimuli
 179 (**Figure 1B**) – *Near Surround* (0.5° diagonally from fixation, 11.6° × 9.2° visual angle) and *Inside*

180 *Border* (1.5° diagonally from fixation). The activation in the early visual areas for the (*Target –*
181 *Near Surround*) contrast is shown in **Figure 1C**.

182 **Experimental Design and Statistical Analysis**

183 Task and procedure

184 We presented scenes on a uniform grey background using MRI compatible goggles
185 (NordicNeuroLab) with 800 × 600 pixel screen resolution, which corresponded to 32° × 24°
186 visual angle. In each experiment there were 8 types of trial (2 scenes in 4 different conditions). In
187 each 12 second trial the stimulus was flashed on and off (200 ms on/ 200 ms off) 28 times (11.6
188 secs + variable fixation to account for uncertainty in timing). This flashing increases the signal to
189 noise ratio compared to continuous presentation (Kay et al., 2008) and gives rise to a greater
190 BOLD response (Boynton et al., 1996). Each trial type was presented sequentially, with the trial
191 order randomized in each sequence. Each sequence lasted 96 seconds (8 × 12 s). A 12 second
192 fixation period was included before and after each sequence of trials. Each experimental run
193 lasted 10 min 48 seconds, containing four trial sequences and two mapping sequences (each
194 mapping sequence consisted of *Target* and two *Surrounds*). There were four experimental runs
195 in total. Thus, each stimulus was shown 16 times per experiment. Subjects' task was to fixate on a
196 central checkerboard and report a fixation colour change with a button press. Subjects pressed a
197 different button depending on whether the colour change occurred during scene 1 or scene 2 (right
198 index and middle fingers respectively). The purposes of the task were to ensure that the subject
199 paid attention to which scene was being shown and to minimize eye movements. In addition, we
200 used eye-tracking to make sure subjects were fixating. Subjects were familiarised with the full
201 non-occluded scenes in a short practice run prior to going into the scanner. This was done to
202 increase subjects' contextual associations and thus increase meaningful feedback when viewing
203 the scenes with reduced information in the experimental trials.

204 After the experimental runs, we performed a polar angle retinotopic mapping procedure to
205 estimate the borders of the early visual areas V1-3. This consisted of a single checkerboard wedge
206 which started in the right horizontal meridian and rotated clockwise (12 rotations per scan, wedge

207 angle: 22.5°, scan time: 13 min 28 sec). For 10 subjects, we also performed an eccentricity
208 mapping procedure. This consisted of an expanding ring which started at the centre and expanded
209 towards the periphery (8 expansions per scan, ring width increased exponentially towards the
210 periphery, scan time: 9 min 12 sec).

211 MRI acquisition

212 We collected MRI data using a 3T Siemens Tim Trio System with a 12-channel head coil.
213 We measured blood oxygen level dependent (BOLD) signals with an echo-planar imaging
214 sequence (echo time: 30 ms, repetition time: 1000 ms, field of view: 210 mm, flip angle: 62°, 18
215 axial slices). The spatial resolution for functional data was 3 mm³. Each experimental run had 648
216 volumes. Retinotopic mapping consisted of 808 volumes (polar angle) or 552 volumes
217 (eccentricity). We positioned 18 slices to maximize coverage of occipital cortex. We recorded a
218 high-resolution 3D anatomical scan (3D Magnetization Prepared Rapid Gradient Echo, 1 mm³
219 resolution, 192 volumes).

220 MRI data processing

221 We corrected functional data for each experimental run and retinotopic mapping runs for
222 slice time (cubic spline interpolation) and 3D motion (Trilinear/Sinc interpolation), temporally
223 filtered (high-pass filtered at 6 cycles with GLM-Fourier, and linearly detrended), and spatially
224 normalized data into Talairach space with BrainVoyager QX 2.8 (Brain Innovation, Maastricht,
225 The Netherlands; Goebel, 2012). We used the anatomical data to create an inflated cortical surface
226 and functional data were overlaid.

227 Voxel selection and analysis

228 Excessive subject movement between runs is likely to affect correspondence between
229 voxels from one run to another. This could introduce noise into our analysis as we selected our
230 region of interest (ROI) based on the averaged functional data of all 4 runs. As described
231 previously (Revina et al., 2018), we calculated an alignment value for each subject by measuring
232 Pearson's correlation in a ROI in the visual cortex between the four functional runs. Correlations

233 were performed in a ROI covering the early visual cortex using intensity values from an
234 anatomical representation of the first volume of the functional data of every run. High correlations
235 would suggest a close anatomical alignment between the 4 runs. The median alignment value
236 across subjects was 98.08% and single subject values ranged from 77.85% to 99.31%. We excluded
237 data from further analysis if the alignment value was below 90%, which applied to three subjects.
238 Furthermore, we excluded any subject with chance level performance in any feedforward
239 condition in single trial analysis (significance above chance was measured using permutation
240 analysis with 1000 trials). The feedforward conditions have bottom-up stimulation and hence
241 there should be a difference in activity patterns. If the scenes could not be decoded in these control
242 conditions in a subject, we excluded them from the analysis, as it suggests that the subject might
243 not have been fixating properly, not paying enough attention, falling asleep, and so on. It would
244 not be meaningful to assess feedback classifier performance (or lack of) in such cases. This
245 excluded a further five subjects. Thus, the following analyses were performed on 21 subjects.

246 We identified the cortical representation of the occluded region using a general linear
247 model (GLM) contrast of the *Target* region against the *Near Surround*, as described previously
248 in Smith & Muckli (2010). The ROI was selected from activation in V1 only. To further minimize
249 spillover activity from neighbouring stimulated areas, we selected voxels from the ROI on the
250 basis of the difference between *Target* and *Near Surround* t-values being greater than 1.

251 *Analyses with extended boundary around the occluded region*

252 To further make sure our findings of scene information in the quadrant were not due to
253 spillover activity from the feedforward surround, we performed a separate analysis with more
254 stringent methods of voxel selection. First of all, we selected our region of interest in BrainVoyager
255 as the contrast of the *Target* mapping region being higher than both the *Near Surround* and the
256 *Inner Border* mapping conditions. In addition, we selected voxels fitting the criteria of $(Target -$
257 $Near Surround) > 1$ and $(Target - Inner Border) > 1$. This helped to restrict voxels to the more
258 peripheral regions and to further minimize any voxels at the inner borders of the quadrant.
259 Analysis showed the same pattern of results and significant decoding between the two scenes in

260 all conditions except Small Bubbles Feedback and Full Feedback (average block analysis,
261 Experiment 1 only).

262 Moreover, we performed another analysis using population receptive field (pRF, Dumoulin
263 and Wandell, 2008) mapping for the subjects which had both the polar angle and eccentricity
264 retinotopic mapping available (Expt 2: n = 4, Expt 3: n = 2, Expt 4: n = 4). Again, this was done
265 to restrict our voxel selection to the quadrant. We only included voxels that were both within the
266 occluded region as defined by pRF and only within our original *Target > Near Surround* ROI as
267 defined in BrainVoyager.

268 Multivariate Pattern Classification Analysis

269 The voxels matching all the above-mentioned criteria for each analysis were entered into
270 the linear classifier (Support Vector Machine [SVM], using the LIBSVM toolbox in MATLAB,
271 Chang and Lin, 2001). For classification analyses, we trained the classifier to decode between the
272 2 scenes in each condition. For cross-classification analyses we trained the classifier to decode
273 between the two scenes on one condition and tested on the other. The classifier used single trial
274 activity patterns (beta values) for training, and was then tested on either “single trial” (ST; 8 trials
275 × 4 sequences = 32 separate trials) or “average block” (AB) activity patterns for each of the 8 trial
276 types (average of the 4 repetitions). In other words, for the average block analysis, the training
277 was the same (single trials of three runs, 32 trials in each run) but the testing was done on the
278 average per stimulus condition of the fourth run. For both types of analyses, we trained the
279 classifier on 3 of the runs and tested on the remaining run (i.e. one-run-out cross-validation).

280 In order to get a robust average and to test how well the classifier would perform when the
281 labels were randomly assigned (described in more detail in Revina et al. 2018), we used
282 bootstrapping and permutation analysis. We bootstrapped the classifier performances 10000
283 times for individual subjects (there were four performances for each condition for each subject
284 due to the one-run-out method on the four runs), to estimate the single subject mean. We then
285 bootstrapped these mean values from individual subjects 10000 times to estimate 95% confidence

286 intervals (CIs) on the group mean. We counted classifier performances as significantly above
287 chance (50%) if the 95% CIs did not contain chance-level performance. We used a permutation
288 test (1000 samples) to compute differences between mean group classifier performances
289 (reported p values not corrected for multiple comparisons), by shuffling the observed values
290 across the conditions, and calculating the absolute differences between the conditions. If the
291 observed difference was in the top 5% of the differences distribution, we considered our
292 conditions to be significantly different from each other.

293 Results

294 Our hypothesis is that the surround stimulation drives higher visual areas with larger
295 receptive fields to send a contextual feedback signal to voxels in V1 responding to the occluded
296 quadrant. We can therefore modify the surround stimulation to learn more about the nature of
297 contextual feedback.

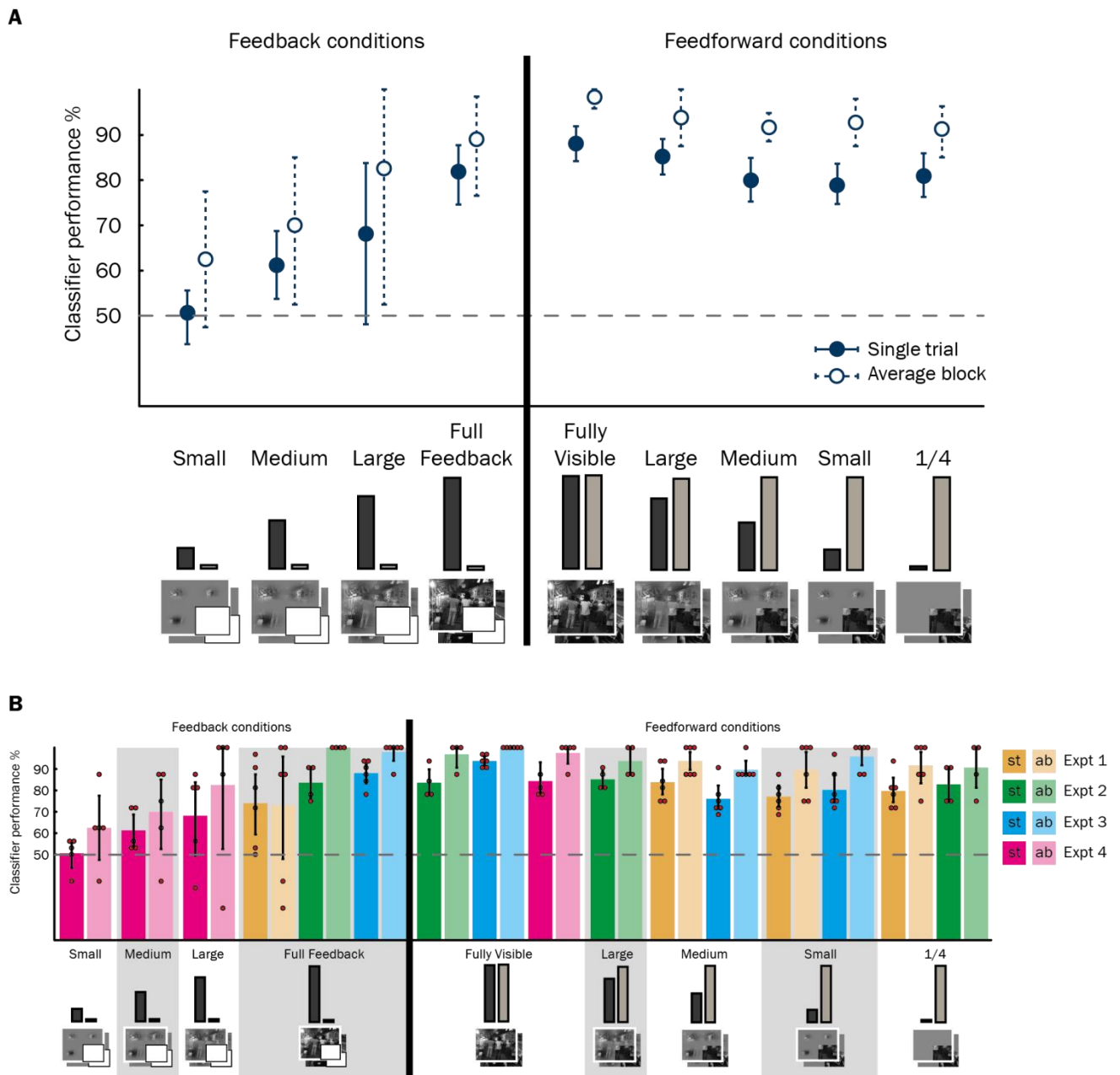
298 **Increased stimulation of the surround receptive field enhances contextual feedback**

299 We have shown previously that scene features eliciting contextual feedback to non-
300 stimulated V1 are not only those features located nearest to the occluded region of the image
301 (Smith and Muckli 2010). That is, voxels contributing information to scene classification are not
302 only found near the border of the occluder (Morgan et al., 2019). This finding suggests that scene
303 classification in non-stimulated voxels is not only related to short-range lateral connections.
304 Expanding on these findings, we assessed the amount of surrounding scene information required
305 to elicit scene-relevant information in non-stimulated V1. We parametrically modulated the
306 availability of surround information and trained the SVM classifier to decode between the two
307 scenes using voxel patterns responding to the lower right quadrant when it was either occluded
308 (feedback and lateral, but no feedforward information) or stimulated (feedforward, feedback and
309 lateral information). SVM classification performance was used as an estimate of the amount of
310 available information in the activation pattern.

311 When the image was occluded, scene classification in non-stimulated voxels improved with
 312 increasing availability of surrounding scene information (**Figure 2A**, left). Averaging across
 313 experiments, classification was significantly above chance once the bubbles exceeded the smallest
 314 size, except for Large Bubbles Single Trial analysis (**Table 1**). Classifier performance for the Full
 315 Feedback condition was significantly higher than the Small or Medium Bubbles conditions
 316 (Small: ST: $p < 0.001$; AB: $p = 0.015$; Medium: ST only: $p = 0.009$). Increased surround
 317 information also improved classifier performance during feedforward processing of the scenes
 318 (**Figure 2A**, right), even though voxels received identical feedforward stimulation. The Fully
 319 Visible condition was significantly higher than the other feedforward conditions (Large: AB only,
 320 $p = 0.019$; Medium: ST: $p = 0.028$, AB: $p = 0.001$; Small: ST only, $p = 0.007$; 1/4: ST: $p = 0.034$,
 321 AB: $p = 0.017$). Classification performance for individual experiments is shown in **Figure 2B**.

322 **Table 1.** Classification performance for decoding between the two scenes in each condition, for feedback and
 323 feedforward stimuli, averaged across experiments.

	Single trial classification	Confidence interval	Average block classification %	Confidence interval
<u>Feedback</u>				
325	Small Bubbles	50.62	0.0687	0.0500
326	Medium Bubbles	61.25	0.0750,	0.0750
	Large Bubbles	68.13	0.1875,	0.1563
327	Full Feedback	81.84	0.0723,	0.0586
<u>Feedforward</u>				
328	Fully Visible	88.12	0.0396,	0.0375
	Large Bubbles	85.16	0.0391,	0.0391
329	Medium Bubbles	79.95	0.0443,	0.0495
	Small Bubbles	78.91	0.0413,	0.0469
	1/4	80.94	0.0469,	0.0500



330

331 **Figure 2.** Classification performance for decoding between the two scenes in each condition, for feedback and
 332 feedforward stimuli. Chance level is 50%. Lines represent 95% confidence intervals around the bootstrapped mean
 333 (10000 bootstrap samples of individual subjects' performances). Classifier performance is significantly above chance
 334 at $\alpha = 0.05$ (not corrected for multiple comparisons) if the confidence intervals do not intersect with the chance line.
 335 A) Classifier performance for each condition, averaged over the four experiments (solid line = classifier tested on
 336 single trials; dashed line = classifier tested on blocks of conditions averaged over the same type). Small, Medium
 337 and Large Feedback conditions, $n = 5$; Full Feedback, $n = 16$; Fully Visible, $n = 15$; Large Feedforward, $n = 4$, Medium
 338 and Small Feedforward, $n = 12$; $\frac{1}{4}$, $n = 10$. B) Same data as in (A) but classifier performance split by four experiments
 339 (separate colours). ST (dark hues) show performance when classifier was tested on single trials; AB (light hues)
 340 when tested on blocks of conditions averaged over the same type. Red circles represent individual subjects' results.

341 Contextual feedback enhances feedforward processing

342 Classifier analyses so far reveal that increased presence of the surrounding scene enhances
 343 scene-specific information in non-stimulated V1. This finding is consistent with the hypothesis
 344 that part of V1 neuronal information patterns comprises feedback signals from areas with larger

345 receptive fields higher up in the visual hierarchy. Interestingly, feedforward information was also
346 enhanced with increased surround stimulation. Observing informative feedback signals with and
347 without feedforward input motivates the question: do feedback and feedforward signals carry the
348 same information? We used a cross-classification approach to test if the classifier can discriminate
349 the two scenes in the feedback conditions and then use this information to discriminate scenes in
350 the feedforward condition. Successful cross-classification would suggest similar information
351 content in feedforward and feedback signals.

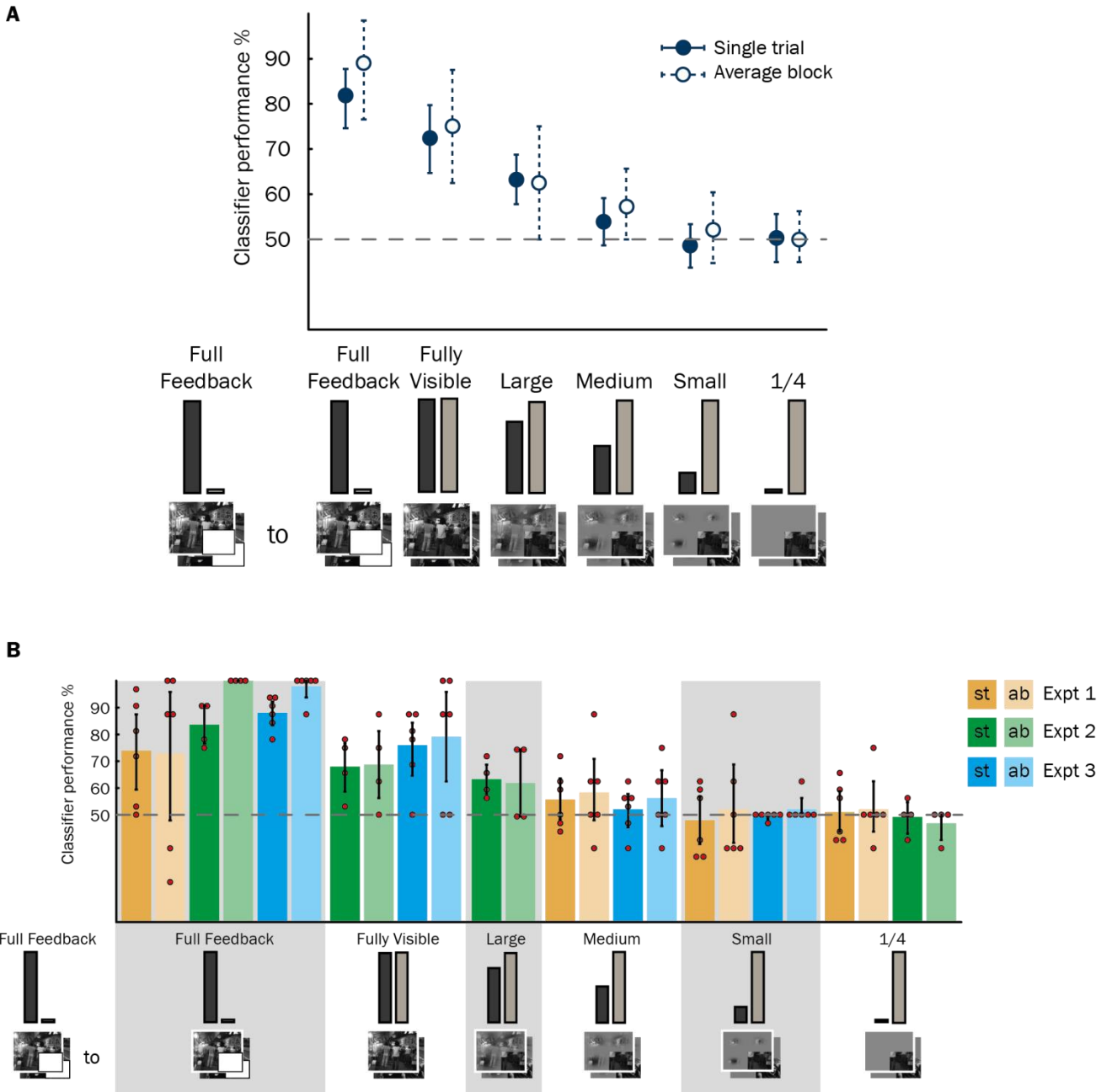
352 How much does feedback contribute to visual processing?

353 We trained the classifier to decode between the two scenes in the Full Feedback condition
354 (with no direct feedforward input in the quadrant) and tested on the feedforward conditions, with
355 varying amount of feedback from the surround (**Figure 3**). Cross-classification performance
356 decreased with decreasing scene information in the surround. The classifier could generalize from
357 the Full Feedback condition to the Fully Visible and Large Bubbles condition (ST only; **Figure**
358 **3A** and **Table 2**). However, cross-classification for Medium, Small Bubbles, and $\frac{1}{4}$ conditions
359 was at chance level. Averaging across experiments (**Figure 3A**), the Fully Visible condition was
360 significantly higher than the Medium Bubbles (ST: $p = 0.002$; AB: $p = 0.021$), Small Bubbles (ST:
361 $p < 0.001$; AB: $p < 0.001$) and the $\frac{1}{4}$ condition (ST: $p < 0.001$; AB: $p = 0.003$). These results tell
362 us that we can train on a feedback signal (that likely has a coarser resolution of information), and
363 test on a signal that is a combination of fine-grained feedforward signal and (coarse) surround
364 feedback signal. This cross-classification must be due to the contextual feedback signal rather
365 than shared information between feedforward and feedback because when the surround stimulus
366 is reduced to nothing (i.e. with shrinking bubbles), we learn that the content of information or its
367 scale (coarse or fine) in feedforward and feedback signals differs.

368

369 **Table 2.** Cross-classification performance for training on the Full Feedback condition and testing on the feedforward
 370 conditions, averaged across experiments.

371		Single trial classification	Confidence interval	Average block classification %	Confidence interval
372	Fully Visible	72.50	0.0781, 0.0750	75.00	0.1125, 0.1125
	Large Bubbles	63.28	0.0547, 0.0547	62.50	0.1250, 0.1250
373	Medium Bubbles	53.91	0.0521, 0.0495	57.29	0.0729, 0.0833
	Small Bubbles	48.70	0.0495, 0.0469	52.08	0.0625, 0.0833
	1/4	50.31	0.0500, 0.0531	50.00	0.0500, 0.0625



374

375 **Figure 3.** Cross-classification performance for training on the Full Feedback condition and testing on the feedforward
 376 conditions. Chance level is 50%. Lines represent 95% confidence intervals around the bootstrapped mean.
 377 Classification performance for the Full Feedback stimulus (training and testing on the same condition) is shown for
 378 comparison. Classifier performance is significantly above chance at $\alpha = 0.05$ (not corrected for multiple comparisons)
 379 if the confidence intervals do not intersect with the chance line. A) Classifier performance for each condition, averaged
 380 over the four experiments (solid line = classifier tested on single trials; dashed line = classifier tested on blocks of
 381 conditions averaged over the same type). Fully Visible, $n = 10$; Large, $n = 4$; Medium and Small, $n = 12$; 1/4, $n = 10$.
 382 B) Same data as in (A) but classifier performance split by four experiments (separate colours). ST (dark hues) show
 383 performance when the classifier was tested on single trials; AB (light hues) when tested on blocks of conditions
 384 averaged over the same type. The small red circles represent individual subjects' results.

385

386

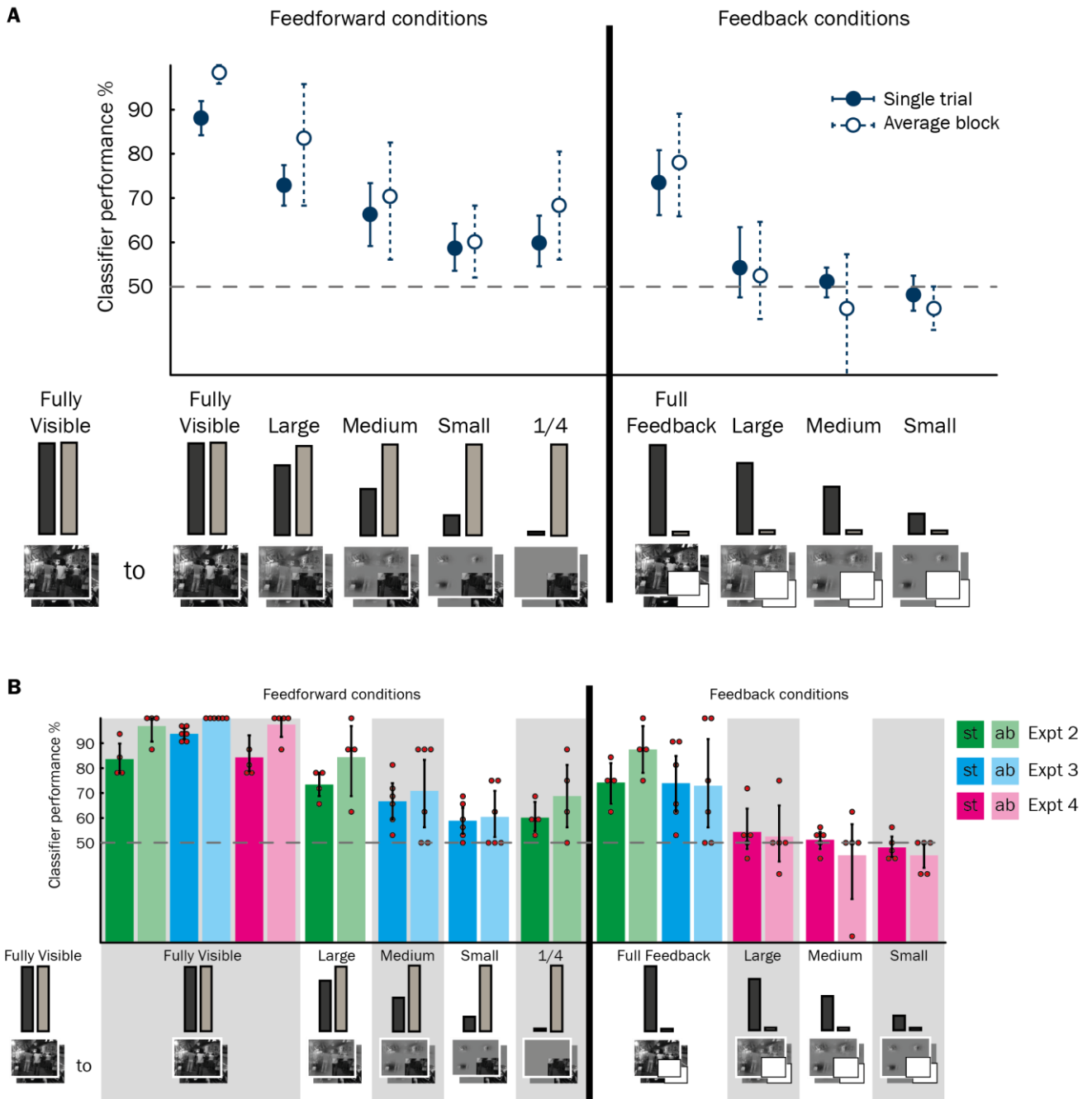
387

To further test how much surround information contributes to visual processing, we compared the Fully Visible scene with other feedforward conditions with a reduced scene surround, as well as the feedback conditions (**Figure 4**). We trained the classifier on the Fully

388 Visible scene and tested on the other conditions. In a fully visible scene both parts of the
 389 information are available simultaneously and the classifier might rely more on the rich, fine-
 390 grained feedforward information. However, we found that Fully Visible feedforward to feedback
 391 cross-classification was only possible with large amounts of scene information surrounding the
 392 occluded region (**Table 3**). Fully Visible to Full Feedback cross-classification was above chance,
 393 while Large, Medium and Small Bubbles did not reach significance in the feedback conditions. In
 394 addition, although we could cross-classify above chance from the Fully Visible to all other
 395 feedforward conditions, cross-classification reduced with decreased scene information in the
 396 surround. Classifier performance was significantly higher for Large Bubbles compared to Small
 397 Bubbles (ST: $p = 0.007$; AB: $p = 0.023$) and $1/4$ (ST only: $p = 0.028$) conditions. If contextual
 398 feedback did not contribute scene-specific information to V1, we would have observed equal cross-
 399 classification across feedforward conditions, regardless of surround stimulation. This suggests
 400 that much of the information in the activity patterns of the Fully Visible scene comes from
 401 feedback from the surround.

402 **Table 3.** Cross-classification performance for training the classifier on the Fully Visible scene and testing on the other
 403 feedforward and feedback conditions, averaged across experiments.

	Single trial classification	Confidence interval	Average block classification %	Confidence interval
<u>Feedforward</u>				
Large Bubbles	73.44	0.0469, 0.0469	84.38	0.1563, 0.1250
Medium Bubbles	66.67	0.0729, 0.0729	70.83	0.1458, 0.1250
Small Bubbles	58.85	0.0521, 0.0573	60.42	0.0833, 0.0833
$1/4$	60.16	0.0547, 0.0625	68.75	0.1250, 0.1250
<u>Feedback</u>				
Full Feedback	74.06	0.0750, 0.0750	78.75	0.1250, 0.1125
Large Bubbles	54.37	0.0687, 0.0938	52.50	0.1000, 0.1250
Medium Bubbles	51.25	0.0375, 0.0313	45.00	0.1750, 0.1250
Small Bubbles	48.13	0.0375, 0.0438	45.00	0.0500, 0.0500



410

411 **Figure 4.** Cross-classification performance for training the classifier on the Fully Visible scene and testing on the
 412 other feedforward and feedback conditions. Chance level is 50%. Lines represent 95% confidence intervals around
 413 the bootstrapped mean. Classification performance for the Fully Visible stimulus (training and testing on the same
 414 condition) is shown for comparison. Classifier performance is significantly above chance at $\alpha = 0.05$ (not corrected
 415 for multiple comparisons) if the confidence intervals do not intersect with the chance line. A) Classifier performance
 416 for each condition, averaged over the four experiments (solid line = classifier tested on single trials; dashed line =
 417 classifier tested on blocks of conditions averaged over the same type). Large Feedforward, $n = 4$; Medium and Small
 418 Feedforward, $n = 6$; $\frac{1}{4}$, $n = 4$; Full Feedback, $n = 10$; Large, Medium and Small Feedback, $n = 5$. B) Same data as in
 419 (A) but classifier performance split by four experiments (separate colours). ST (dark hues) show performance when
 420 the classifier was tested on single trials; AB (light hues) when tested on blocks of conditions averaged over the same
 421 type. The small red circles represent individual subjects' results.

422

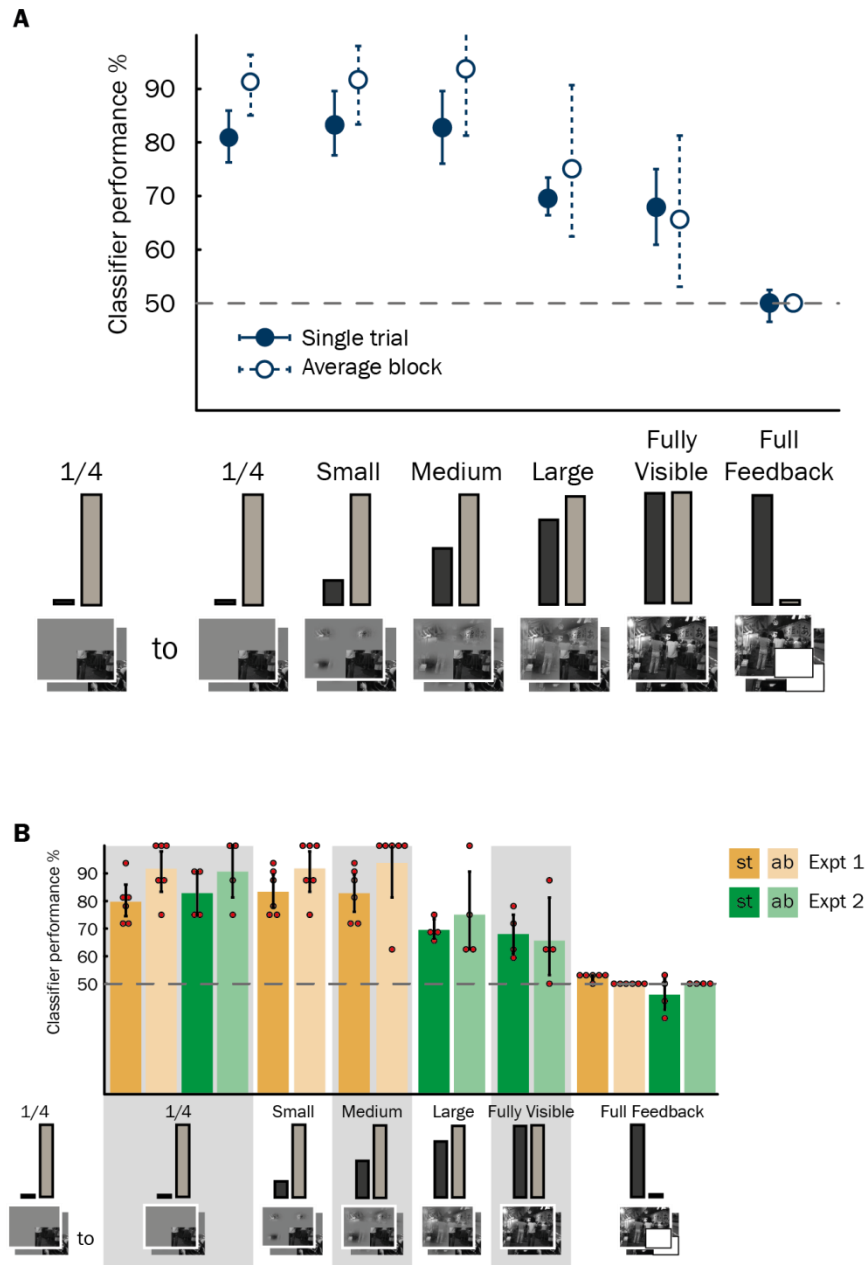
423 Interestingly, we found that when the classifier was trained on the Fully Visible image
 424 (**Figure 4**) it cross-classified better to Full Feedback than to feedforward conditions in which the

425 feedback was restricted by reduced contextual information (significantly above chance for Small
 426 Bubbles: ST: $p = 0.013$; AB: $p = 0.035$). This suggests that feedback in the occluded region from
 427 full stimulation in the surround is at least as informative about the scene as feedforward
 428 information in the quadrant with minimal surround stimulation. This shows that feedback is an
 429 important part of the information in V1, both when feedforward stimulation is present and when
 430 it is absent.

431 If surround feedback information interacts with feedforward processing, then increasing
 432 contextual surround information should reduce cross-classification from the 1/4 feedforward
 433 condition to feedforward conditions with surround stimulation (**Figure 5**). Indeed, cross-
 434 classifier performance for 1/4 to Small Bubbles (**Table 4**) was higher than to Large (ST only: $p =$
 435 0.015) or the Fully Visible condition (ST: $p = 0.021$; AB: $p = 0.006$). Cross-classifier performance
 436 for 1/4 to Medium Bubbles was also significantly higher than to Large (ST only: $p = 0.039$) or the
 437 Fully Visible condition (ST: $p = 0.037$; AB: $p = 0.036$).

438 **Table 4.** Cross-classification performance for training the classifier on the 1/4 and testing on the other feedforward
 439 conditions, averaged across experiments.

	Single trial classification	Confidence interval	Average block classification %	Confidence interval
Small Bubbles	83.33	0.0573, 0.0625	91.67	0.0833, 0.0625
Medium Bubbles	82.81	0.0677, 0.0677	93.75	0.1250, 0.0625
Large Bubbles	69.53	0.0313, 0.0391	75.00	0.1250, 0.1563
Fully Visible	67.97	0.0703, 0.0703	65.63	0.1250, 0.1563



440

441 **Figure 5.** Cross-classification performance for training the classifier on the $\frac{1}{4}$ condition and testing on the other
 442 feedforward and feedback conditions. Chance level is 50%. Lines represent 95% confidence intervals around the
 443 bootstrapped mean. Classification performance for the $\frac{1}{4}$ stimulus (training and testing on the same condition) is
 444 shown for comparison. Classifier performance is significantly above chance at $\alpha = 0.05$ (not corrected for multiple
 445 comparisons) if the confidence intervals do not intersect with the chance line. A) Classifier performance for each
 446 condition, averaged over the four experiments (solid line = classifier tested on single trials; dashed line = classifier
 447 tested on blocks of conditions averaged over the same type). Small and Medium, $n = 6$; Large and Fully Visible, $n =$
 448 4; Full Feedback, $n = 10$. B) Same data as in (A) but classifier performance split by four experiments (separate
 449 colours). ST (dark hues) show performance when the classifier was tested on single trials; AB (light hues) when
 450 tested on blocks of conditions averaged over the same type. The small red circles represent individual subjects'
 451 results.

452 Does increased presentation of the entire image change feedback information?

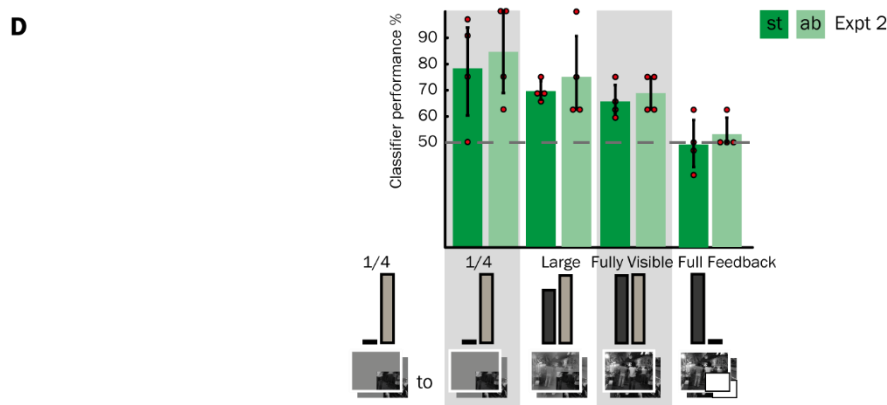
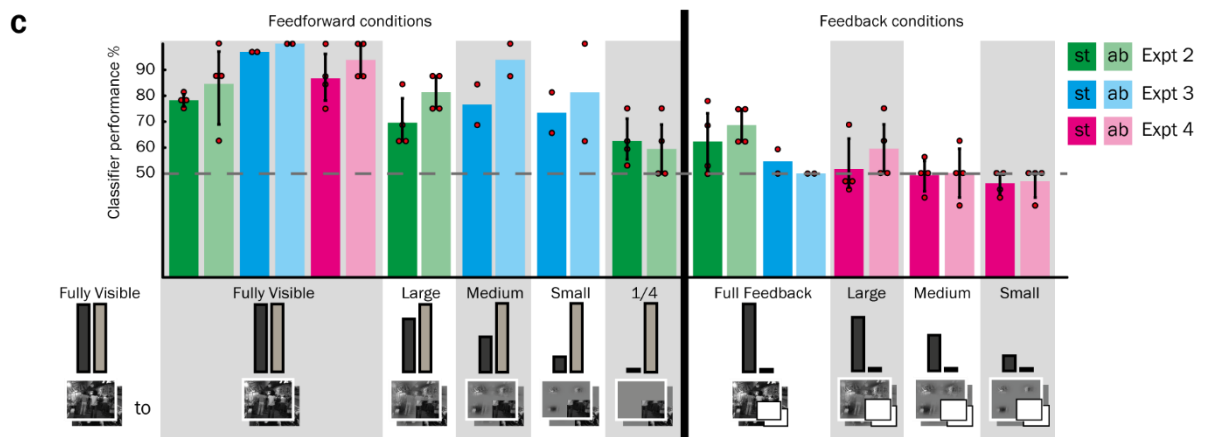
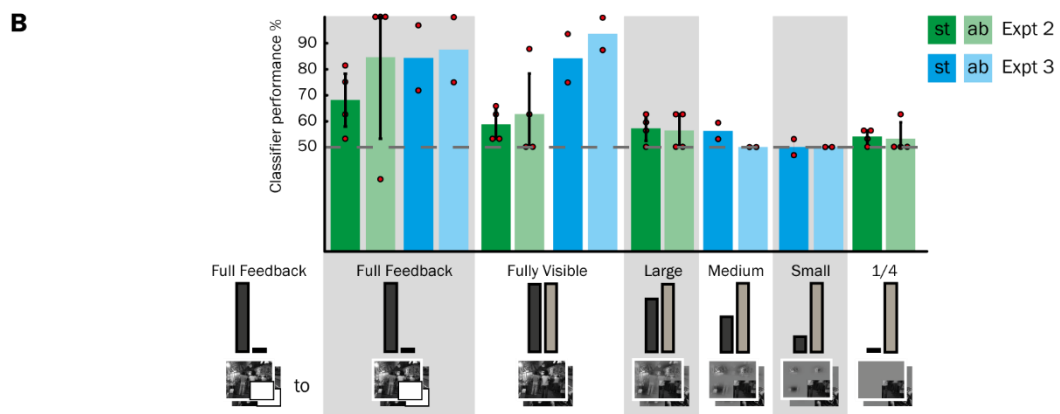
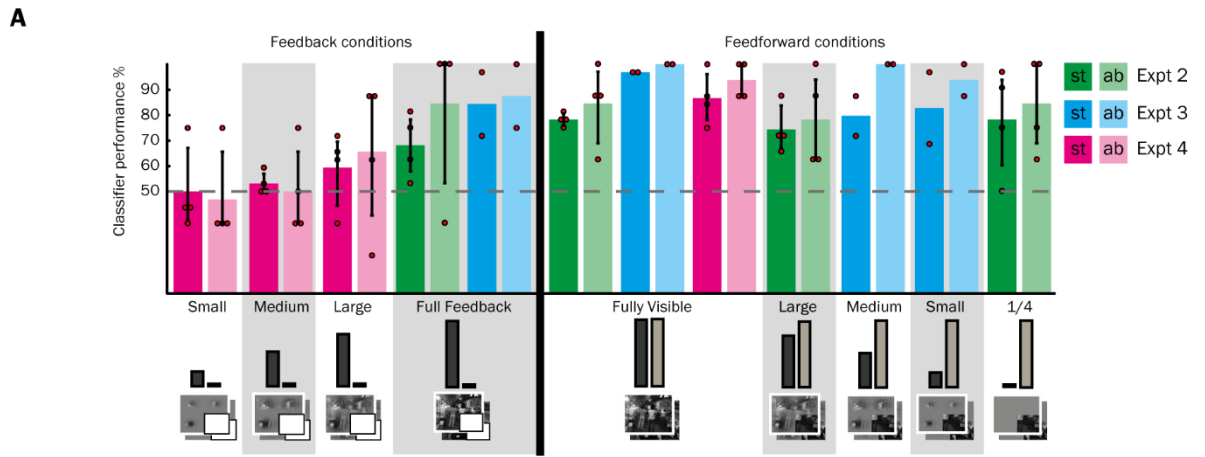
453 Apart from varying how much surround information is visible in a stimulus, we also
 454 investigated whether knowledge of the full scene would improve feedback in the stimuli with
 455 reduced surround. In Experiment 3, we presented the Fully Visible scenes along with the Medium

456 and Small Bubbles stimuli, unlike in Experiment 1 where we had not presented the Fully Visible
457 scene as one of the stimuli (although all subjects were shown the full scenes in a practice run prior
458 to the experimental session). Varying the frequency of the Fully Visible scene allowed us to
459 investigate whether being presented with the full structure of the scene (during the experimental
460 run) would boost meaningful feedback in stimuli with reduced surround information. We found
461 that cross-classification from Full Feedback to Small and Medium Bubbles was at chance level for
462 both Experiment 1 and 3 (**Figure 3B**), suggesting that reduced feedback to the feedforward
463 quadrant in the Small and Medium Bubbles stimuli was mainly due to the decreased contextual
464 surround information in the stimulus as opposed to a reduced implicit memory of the fully visible
465 scene.

466 **Results with extended safety boundary around occluded region**

467 We performed an additional separate analysis in order to decrease the number of voxels
468 that are close to the boundary region and hence reduce the possibility of any feedforward
469 stimulation “spilling over” from the surround. For the conjunction analysis using the contrast of
470 (*Target > Near Surround*) & (*Target > Inner Border*), we found the same pattern of results and
471 significant decoding between the two scenes in all conditions except Small Bubbles Feedback, and
472 Full Feedback (AB analysis, Experiment 1 only).

473 After restricting voxels to the occluded region using pRF mapping, we saw that classifier
474 performance decreased in some conditions, but the pattern of the results remained the same
475 (**Figure 6**). Due to the low numbers of subjects in each experiment for whom we were able to
476 perform pRF mapping, we did not calculate confidence intervals for some of the mean values.



478 **[Previous page] Figure 6.** Classification and cross-classification performance after applying population receptive
479 field (pRF) mapping to further constrain voxels to the occluded region. Classifier performance is shown for each
480 condition for each of the three experiments (separate colours; Expt 2: n = 4; Expt 3: n = 2; Expt 4: n = 4). ST (dark
481 hues) show performance when the classifier was tested on single trials; AB (light hues) when tested on blocks of
482 conditions averaged over the same type. The small red circles represent individual subjects' results. Chance level is
483 50%. A) Decoding two scenes in the same condition. B) Training on Full Feedback and testing on feedforward
484 conditions. C) Training on the Fully Visible scene and testing on other feedforward and feedback conditions. D)
485 Training on the $\frac{1}{4}$ condition and testing on other feedforward and feedback conditions.

486

487 Discussion

488 We studied the influence of the scene surround on populations of neurons using fMRI,
489 complementing what we know from electrophysiology studies investigating classical and non-
490 classical neuronal receptive fields. We established that the availability of contextual information
491 affects cortical feedback to a non-stimulated region in V1. Specifically, the extent of contextual
492 modulation in non-stimulated V1 depends on the amount of scene information surrounding the
493 occluded image quadrant. Furthermore, information in the non-stimulated region does not
494 represent a direct filling-in of missing feedforward input, and that contextual feedback enhances
495 information in V1 even when rich feedforward information is available.

496 V1 neurons integrate signals over a large area beyond the classical receptive field
497 (Angelucci et al., 2002; Angelucci and Bressloff, 2006). Lateral connections modulate the
498 response in the central receptive field over short distances. However, feedback from higher areas
499 accounts for the full extent of the surround modulation effects (Angelucci and Bressloff, 2006).
500 There was no meaningful feedforward stimulation in our occluded region of V1, and yet we could
501 decode two scenes using information patterns corresponding to this non-stimulated region. This
502 differential information must originate from contextual information in the scene surround.
503 Classical receptive fields are smaller than the surround, hence neurons in the occluded area in V1
504 most likely receive information about the rest of the scene via cortical feedback from higher areas.
505 Since we are measuring a population of neurons using fMRI, as opposed to single cells, it is hard
506 to estimate how widespread the effect of the surround receptive field is. V1 receives feedback from
507 many cortical areas, which have increasing receptive field sizes moving to higher and more
508 abstract processing areas (Dumoulin and Wandell, 2008). Therefore, we expect that influence

509 from the surround might be restricted to regions close to the occluded region for feedback coming
510 from V2, for example, but transmit information from a larger area of the surrounding scene for
511 feedback originating from higher visual areas.

512 We found that larger bubbles in the surround lead to more informative feedback in the
513 occluded region. This may be because we are revealing more of the overall scene structure as we
514 increase the bubble size. Tang and colleagues (2014) demonstrated top-down effects in image
515 completion by presenting partially revealed images using bubbles. The number of bubbles was
516 constant, but their location was changed. This suggests that revealing a certain amount of the
517 global image structure, regardless of the specific parts, can be enough for top-down completion
518 to take effect. Alternatively, our result could be explained by larger bubbles providing more
519 information close to the lower right quadrant, compared to small bubbles, because our bubbles
520 were centred in each quadrant. However, Williams and colleagues (2008) have demonstrated that
521 feedback can come from distant retinotopic regions, by showing that the fovea receives feedback
522 about objects in the periphery. Since we did not specifically measure effects of bubble location, it
523 remains to be seen how varying proximity of surrounding information affects feedback
524 information in non-stimulated V1. It also remains to be seen how contextual feedback depends on
525 the presence of task-specific diagnostic features that could be revealed on different trials using
526 bubbles (Gosselin and Schyns, 2001). Subsets of stimulus features drive information states of
527 functionally-relevant higher brain regions (e.g. face areas) during the feedforward sweep of visual
528 processing (e.g. Schyns et al., 2007) and these representations could modulate the content of
529 cortical feedback signals. For the purpose of this study we kept these parameters constant.

530 **Interaction of feedback and feedforward signals**

531 We found that stimulating the surround increased information in both the occluded region
532 and when it contains feedforward information. Similarity between identical feedforward
533 quadrants was reduced if the amount of information in the surround was increased. If feedback
534 signals from the surround did not combine with feedforward information or only weakly
535 modulated it, we would have seen similar activity patterns relating to the feedforward quadrant

536 regardless of the surround. The feedforward signal has been traditionally considered the
537 dominant signal, since it drives receptive fields, while feedback has been thought of mostly
538 modulatory and not necessarily able to trigger spikes (Bullier, 2006; Bastos et al., 2012), but see
539 Mignard and Malpeli, (1991). By using fMRI which is also sensitive to non-spiking activity
540 (Logothetis, 2008; Muckli, 2010) we established that this modulation from feedback may be just
541 as important as the spiking produced by stimuli in a bottom-up manner. fMRI is sensitive to
542 postsynaptic inputs including the arrival of feedback onto the apical dendrites. Feedback can be
543 combined with feedforward inputs arriving to the basal dendrites, meaning that individual
544 neurons integrate internally-generated feedback signals with sensory-derived feedforward signals
545 (Larkum, 2013), a process which might be a cornerstone of conscious perception (Phillips et al.,
546 2016). Though this neuronal mechanism remains to be observed in the visual cortex, many studies
547 support the notion that feedback to V1 is a crucial part of visual perception. For example, reducing
548 feedback from higher areas such as V2, MT or hMT reduces the neuronal response the lower areas
549 to visual stimulation in the centre RF, (Sandell and Schiller, 1982; Hupé et al., 1998, 2001;
550 Schmidt et al., 2011) and in humans affects prediction in an apparent motion paradigm (Vetter et
551 al., 2015).

552 **Information content of feedback**

553 Predictive coding theories (Rao and Ballard, 1999; Friston, 2010; Clark, 2013) hypothesise
554 that the occluded part of our scenes should be represented in non-stimulated cortex, based on the
555 expected scene structure behind the occluder. Several authors have demonstrated that an
556 expected or predicted stimulus evokes activity in V1 which is similar to activity elicited by actual
557 bottom-up stimulation (e.g. Ban et al., 2013; Gavornik and Bear, 2014; Kok et al., 2014).
558 Therefore, at first glance, it is surprising that we do not find similarity between the occluded
559 region and the missing feedforward quadrant. This suggests information in feedback signals does
560 not represent a direct filling-in of the missing feedforward input. However, a lack of a direct
561 filling-in is not so counter-intuitive since participants do not report seeing the missing portion of
562 the scene in occluded trials (i.e. they do not have a hallucination). Hence feedback and

563 feedforward information may be coded in different formats, even though both carry information
564 about the scene. For example, it may be that information is coarser in terms of its content because
565 of the larger visual fields in higher visual areas or less precise retinotopically (e.g. de-Wit et al.,
566 2012). Alternatively, feedback may provide a more abstract version of the scene. In a previous
567 study, we have shown that feedback information is comparable to a line drawing completing the
568 missing quadrant (Morgan et al., 2019). Finally, a difference in neural patterns could be observed
569 because feedback and feedforward signals project to different cortical layers (Rockland and Virga,
570 1989; Muckli et al., 2015). Muckli and colleagues (2015) showed using high-resolution fMRI that
571 during normal visual stimulation, feedforward information peaks in mid-layers of V1, while
572 contextual feedback information peaks in the superficial layers. Recent data from neural network
573 modelling also suggests that recurrent processing is not completing or filling-in the information
574 to make it identical to the feedforward response, but rather it may function by suppressing
575 occluders and enhancing responses to the hidden target (Spoerer et al., 2017). Recurrent networks
576 also outperform feedforward models in identifying the occluded target stimulus, suggesting that
577 feedback enhances feedforward processing.

578 If feedback signals are carrying expectations and predictions based on prior knowledge we
579 might find that improved knowledge of the full scene structure would be important for meaningful
580 feedback in the occluded region. However, it seems that knowledge about the particular scene
581 being viewed is not necessary. Smith and Muckli (2010) previously found that contextual feedback
582 in the occluded region is present even if participants never see the fully visible scene and were not
583 familiarised with it. We also found that increased exposure to the full scene did not improve
584 feedback in the conditions with reduced surround. Therefore, it appears that the contextual
585 feedback we observed arises from the scene structure available in each trial, or knowledge of
586 natural scene properties in general, but familiarity with the specific scene is not required for
587 informative feedback signals. This could be because natural scenes have predictable scene
588 statistics and much of the information they contain is redundant (e.g. Attneave, 1954; Barlow,
589 1961; Torralba and Oliva, 2003).

590 Conclusion

591 We demonstrated that cortical feedback information forms a part of early visual cortex
592 activity during visual stimulation. Using a brain imaging technique we have corroborated
593 evidence from animal electrophysiology showing that stimulation in the far-surround receptive
594 field modulates responses in the classical visual receptive field. We show that increased
595 information in the scene surround results in increased scene information in both stimulated and
596 non-stimulated visual field regions. We conclude that cortical feedback carries abstract internal
597 models of natural scenes which are combined with more spatially-specific, detailed
598 representations in primary visual cortex, and that the merging of high-level content of cortical
599 feedback with feedforward signals should constrain our understanding of cortical function during
600 perception.

601 References

- 602 Angelucci A, Bressloff PC (2006) Contribution of feedforward, lateral and feedback connections to the
603 classical receptive field center and extra-classical receptive field surround of primate V1 neurons.
604 Progress in Brain Research 154:93–120.
- 605 Angelucci A, Levitt JB, Walton EJS, Hupé J-M, Bullier J, Lund JS (2002) Circuits for local and global
606 signal integration in primary visual cortex. The Journal of Neuroscience 22:8633–8646.
- 607 Attneave F (1954) Some informational aspects of visual perception. Psychological Review 61:183–193.
- 608 Ban H, Yamamoto H, Hanakawa T, Urayama S, Aso T, Fukuyama H, Ejima Y (2013) Topographic
609 representation of an occluded object and the effects of spatiotemporal context in human early
610 visual areas. The Journal of Neuroscience 33:16992–17007.
- 611 Bar M (2004) Visual objects in context. Nature Reviews Neuroscience 5:617–629.
- 612 Barlow HB (1961) The coding of sensory messages. In Thorpe WH, Zangwill OL, (eds) Current
613 Problems in Animal Behaviour. Cambridge: University Press.
- 614 Bastos AM, Usrey WM, Adams RA, Mangun GR, Fries P, Friston KJ (2012) Canonical microcircuits for
615 predictive coding. Neuron 76:695–711.

- 616 Boynton GM, Engel SA, Glover GH, Heeger DJ (1996) Linear systems analysis of functional magnetic
617 resonance imaging in human V1. *The Journal of Neuroscience* 16:4207–4221.
- 618 Bullier J (2006) What is fed back? In: *23 Problems in Systems Neuroscience* (van Hemmen JL,
619 Sejnowski TJ, eds) Oxford Scholarship Online. Oxford; New York: Oxford University Press.
- 620 Clark A (2013) Whatever next? Predictive brains, situated agents, and the future of cognitive science.
621 *Behavioral and Brain Sciences* 36:181–204.
- 622 de-Wit LH, Kubilius J, Wagemans J, Op de Beeck HP (2012) Bistable Gestalts reduce activity in the
623 whole of V1, not just the retinotopically predicted parts. *Journal of Vision* 12:12.
- 624 Douglas RJ, Martin KA (2007) Mapping the matrix: the ways of neocortex. *Neuron* 56:226–238.
- 625 Dumoulin SO, Wandell BA (2008) Population receptive field estimates in human visual cortex.
626 *NeuroImage* 39:647–660.
- 627 Friston K (2010) The free-energy principle: a unified brain theory? *Nature Reviews Neuroscience*
628 11:127–138.
- 629 Gavornik JP, Bear MF (2014) Learned spatiotemporal sequence recognition and prediction in primary
630 visual cortex. *Nature Neuroscience* 17:732–737.
- 631 Gilbert CD, Li W (2013) Top-down influences on visual processing. *Nature Reviews Neuroscience*
632 14:350–363.
- 633 Gilbert CD, Sigman M (2007) Brain states: top-down influences in sensory processing. *Neuron* 54:677–
634 696.
- 635 Goebel R (2012) BrainVoyager — Past, present, future. *NeuroImage* 62:748–756.
- 636 Gosselin F, Schyns PG (2001) Bubbles: a technique to reveal the use of information in recognition tasks.
637 *Vision Research* 41:2261–2271.
- 638 Hupé J-M, James AC, Payne BR, Lomber SG, Girard P, Bullier J (1998) Cortical feedback improves
639 discrimination between figure and background by V1, V2 and V3 neurons. *Nature* 394:784–787.
- 640 Kay K, Naselaris T, Prenger R, Gallant J (2008) Identifying natural images from human brain activity.
641 *Nature* 452:352–355.

- 642 Kok P, Failing MF, de Lange FP (2014) Prior expectations evoke stimulus templates in the primary visual
643 cortex. *Journal of Cognitive Neuroscience* 26:1546–1554.
- 644 Larkum M (2013) A cellular mechanism for cortical associations: an organizing principle for the cerebral
645 cortex. *Trends in Neurosciences* 36:141–151.
- 646 Larkum ME, Petro LS, Sachdev RNS, Muckli L (2018) A perspective on cortical layering and layer-
647 spanning neuronal elements. *Frontiers in Neuroanatomy* 12:56.
- 648 Li W, Piëch V, Gilbert CD (2004) Perceptual learning and top-down influences in primary visual cortex.
649 *Nature Neuroscience* 7:651-657.
- 650 Logothetis NK (2008) What we can do and what we cannot do with fMRI. *Nature* 453:869–878.
- 651 Mignard M, Malpeli JG (1991) Paths of information flow through visual cortex. *Science* 251:1249–1251.
- 652 Morgan AT, Petro LS, Muckli L (2019) Scene representations conveyed by cortical feedback to early
653 visual cortex can be described by line drawings. *The Journal of Neuroscience* 39:9410–9423.
- 654 Muckli L (2010) What are we missing here? Brain imaging evidence for higher cognitive functions in
655 primary visual cortex V1. *International Journal of Imaging Systems and Technology* 20:131–139.
- 656 Muckli L, De Martino F, Vizioli L, Petro LS, Smith FW, Ugurbil K, Goebel R, Yacoub E (2015) Contextual
657 feedback to superficial layers of V1. *Current Biology* 25:2690–2695.
- 658 Petro LS, Muckli L (2018) Forecasting faces in the cortex: comment on “High-level prediction signals in a
659 low-level area of the macaque face-processing hierarchy”, by Schwiedrzik and Freiwald, *Neuron*
660 (2017). *Trends in Cognitive Sciences* 22:95–97.
- 661 Phillips WA, Larkum ME, Harley CW, Silverstein SM (2016) The effects of arousal on apical amplification
662 and conscious state. *Neuroscience of Consciousness* 2016:niw015.
- 663 Rao RP, Ballard DH (1999) Predictive coding in the visual cortex: a functional interpretation of some
664 extra-classical receptive-field effects. *Nature Neuroscience* 2:79–87.
- 665 Revina Y, Petro LS, Muckli L (2018) Cortical feedback signals generalise across different spatial
666 frequencies of feedforward inputs. *NeuroImage* 180:280–290.

- 667 Rockland KS, Virga A (1989) Terminal arbors of individual “feedback” axons projecting from area V2 to
668 V1 in the macaque monkey: a study using immunohistochemistry of anterogradely transported
669 Phaseolus vulgaris-leucoagglutinin. *The Journal of Comparative Neurology* 285:54–72.
- 670 Sandell JH, Schiller PH (1982) Effect of cooling area 18 on striate cortex cells in the squirrel monkey.
671 *Journal of Neurophysiology* 48:38–48.
- 672 Schmidt KE, Lomber SG, Payne BR, Galuske RAW (2011) Pattern motion representation in primary
673 visual cortex is mediated by transcortical feedback. *NeuroImage* 54:474–484.
- 674 Schwiedrzik CM, Freiwald WA (2017) High-level prediction signals in a low-level area of the macaque
675 face-processing hierarchy. *Neuron* 96:89–97.e4.
- 676 Schyns PG, Petro LS, Smith ML (2007) Dynamics of visual information integration in the brain for
677 categorizing facial expressions. *Current Biology* 17:1580–1585.
- 678 Shushruth S (2011) The role of extrastriate feedback in contextual computations in the primate primary
679 visual cortex. Doctoral Thesis. University of Utah.
- 680 Smith FW, Muckli L (2010) Nonstimulated early visual areas carry information about surrounding context.
681 *Proceedings of the National Academy of Sciences* 107:20099–20103.
- 682 Spoerer CJ, McClure P, Kriegeskorte N (2017) Recurrent convolutional neural networks: a better model
683 of biological object recognition. *Frontiers in Psychology* 8:1551.
- 684 Sugita Y (1999) Grouping of image fragments in primary visual cortex. *Nature* 401:269–272.
- 685 Tang H, Buia C, Madhavan R, Crone NE, Madsen JR, Anderson WS, Kreiman G (2014) Spatiotemporal
686 dynamics underlying object completion in human ventral visual cortex. *Neuron* 83:736–748.
- 687 Torralba A, Oliva A (2003) Statistics of natural image categories. *Network* 14:391–412.
- 688 Vetter P, Grosbras M-H, Muckli L (2015) TMS over V5 disrupts motion prediction. *Cerebral Cortex*
689 25:1052–1059.
- 690 Williams MA, Baker CI, Op de Beeck HP, Shim WM, Dang S, Triantafyllou C, Kanwisher N (2008)
691 Feedback of visual object information to foveal retinotopic cortex. *Nature Neuroscience* 11:1439–
692 1445.